Suppressing Impacts of the Amazonian Deforestation by the Global Circulation Change

Tsing-Chang Chen, Jin-ho Yoon, Kathryn J. St. Croix, and Eugene S. Takle
Atmospheric Science Program, Department of Geological and Atmospheric Sciences, Iowa State University, Ames, Iowa

ABSTRACT

Analyzing the Global Historical Climatology Network, outgoing longwave radiation, and NCEP–NCAR reanalysis data over the Amazon Basin, the authors find a clear interdecadal increasing trend over the past four decades in both rainfall and intensity of the hydrological cycle. These interdecadal variations are a result of the interdecadal change of the global divergent circulation. On the contrary, the impact of the Amazon deforestation as evaluated by all numerical studies has found a reduction of rainfall and evaporation, and an increase of temperature in the Amazon Basin extending its dry season. Evidently, the interdecadal trend of the basin's hydrological cycle revealed from observations functions in a course opposite to the deforestation scenario. Results of this study suggest that future studies analyzing the impact of the basin-scale deforestation on the regional hydrological cycle and climate should be reassessed with multidecade numerical simulations including both schemes handling the land-surface processes and the mechanism generating proper interdecadal variation of the global divergent circulation.

1. Introduction

Salati and Nobre (1990), in a review of the basin-scale water vapor budget of the Amazon Basin analyzed by previous studies, pointed out that evapotranspiration accounts for more than 50% of precipitation. This estimate was later confirmed by Nobre et al. (1991) using the water vapor budget of several studies with various horizontal scales within the Amazon Basin. Note that total evapotranspiration was used for these budget analyses. Actually, only a portion of local evapotranspiration is consumed to maintain local precipitation. The ratio between them is referred to as *precipitation recycling,* which is an indicator of the importance of land-surface processes in the water balance of the region. With this approach, Eltahir and Bras (1994) showed that about 25%–35% of the rain within the Amazon Basin (over scales of 2500 km) is contributed by evapotranspiration. Using Brubaker et al.'s (1993) simplified rectangular domain, Trenberth (1999) estimated that roughly 34% of the moisture is recycled over the Amazon Basin.

Regardless of the precipitation recycling estimated either with total evapotranspiration in the convectional water vapor budget analysis, or with only the portion usable in precipitation recycling as Brubaker et al.'s (1993) argument, all available observational evidence seems to suggest that the Amazonian rainforest is highly effective in recycling precipitation into the atmosphere. It follows that replacing the rainforest by the degraded pasture cover will markedly reduce this highly efficient evapotranspiration. Based on several sources (Instituto Nacional de Pesquisas Espaciais 1989; Fearnside 1987; Fearnside 1990; Skole et al. 1990), Nobre et al. (1991, their Fig. 1) estimated that with the current deforestation rate most of the Amazon rainforest would disappear in less than 100 years. Numerous numerical simulations (e.g., Dickinson and Henderson-Sellers 1988; Shukla et al. 1990; Nobre et al. 1991; Henderson-Sellers et al. 1993; Sud et al. 1996; Lean et al. 1996; and many others) using global climate models predict that when all of the Amazon rainforest is replaced by pasture, there will be

Corresponding author address: Tsing-Chang (Mike) Chen, Atmospheric Science Program, Department of Geological and Atmospheric Sciences, Iowa State University, Ames, IA 50011.
E-mail: tmchen@iastate.edu
In final form 4 May 2001.

higher surface temperature (to extend the dry season) and less evaporation and rainfall. These hydrological changes after a massive deforestation may make reforestation difficult over the Amazon Basin.

Analyzing the National Oceanic and Atmospheric Administration's (NOAA) outgoing longwave radiation (OLR) for the period 1974–90 over the Amazon Basin, Chu et al. (1994) found little indication of a decrease in rainfall associated with deforestation. Simulations of shallow convective clouds and precipitation induced by land-surface forcing by Avissar and Liu (1996) seem to indicate that the deforestation at the mesoscale dimension, as is currently occurring in Amazonia, increases the recycling of water, instead of reducing precipitation. Precipitation trends over land for the past century compiled by Easterling et al. (2000, their Fig. 11) and the Intergovernmental Panel on Climate Change report (Houghton et al. 1998, their Fig. 3.7) showed precipitation increases over most of the Amazon Basin. In spite of the fact that deforestation in the Amazon has not yet reached a continental scale, the aforementioned precipitation trends seem to proceed in a direction opposite to the prediction of deforestation simulations by numerical models. What may be the cause of the increasing trend in the Amazon rainfall and why do numerical models show the opposite behavior?

It is revealed from distributions of OLR (e.g., Liebman and Hartmann 1982) and rainfall (Xie and Arkin 1997) that the major tropical convection activity rainfall occurs over the three tropical continents: tropical South America, equatorial Africa, and the maritime continent. Major tropical convection–rainfall centers are coupled with upward branches of the east–west circulation (Krishnamurti et al. 1973). By use of the potential function of water vapor transport and the divergent component of water vapor flux, Chen (1985) was able to demonstrate the maintenance of convection–rainfall centers over the three tropical continents by the water vapor flux convergence, which is driven by the east–west circulation. Evidently, rainfall–convection over the Amazon Basin is linked to the global circulation. Conceivably, the increasing rainfall trend in this basin could be a result of the change in the global circulation. On the other hand, any possible rainfall reduction caused by the deforestation (if possible, as numerical simulations suggested) should also be reflected by the global circulation change. An effort is made in this study to clarify these speculations with several data sources: the National Centers for Environmental Prediction (NCEP)–National Center for Atmospheric Research (NCAR) reanalysis data (Kalnay et al. 1996), the Global Historical Climatological Network (GHCN) station precipitation (Easterling et al. 1996), pressure (Vose et al. 1992) and temperature (Peterson and Vose 1997), sea surface temperature (SST; Smith and Reynolds 1998), and NOAA's OLR.

2. Interdecadal trends

The geography–orography in the northern part of South America is shown in Fig. 1, which includes the GHCN stations [precipitation (P), surface pressure (p_s), and temperature (T_s) denoted by blue dots, open

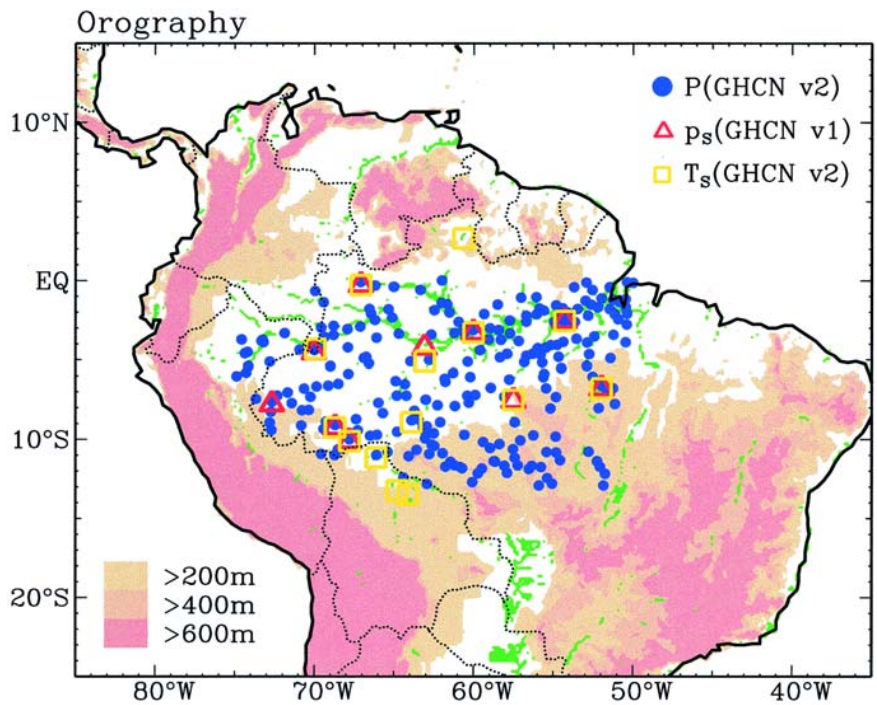

FIG. 1. The geography–orography (dark line/colored area) of northern South America and Global Historical Climatology Network (GHCN) stations below the elevation of 200 m; observations of precipitation (P), surface pressure (p_s), and surface temperature (T_s) are marked by blue dots, red triangles, and yellow squares, respectively.

red triangles, and open yellow squares, respectively] with their elevations below 200 m around the Amazon River. Interdecadal trends of station variables (P, p_s, and T_s), OLR, and reanalysis data {precipitable water (W), convergence of water vapor flux ($-\nabla \cdot \boldsymbol{Q}$), p_s, and convergence at 850 mb [$-\nabla \cdot \boldsymbol{V}$(850 mb)]} within a rectangular domain (15°S–15°N,70°N–50°W) embedded in the Amazon Basin are analyzed with the following procedures.

1) Values of a given variable are added together and averaged over all stations in Fig. 1.
2) OLR and the selected reanalysis variables are averaged individually over the analysis domain.
3) The interdecadal trend of variables shown in Fig. 2 is determined by a linear fit with the statistical scheme described in our previous study (Chen et al. 1996) dealing with the interdecadal variation in the U.S. Pacific coast precipitation over four decades (1950–94).

Rainfall (Fig. 2a) and convection [as indicated by ΔOLR (= $\overline{\text{OLR}}$ – OLR; $\overline{\ }$ multisummer-mean OLR] over the Amazon Basin exhibit an increasing trend over 1950–90 and 1970–99, respectively. Interdecadal trends of these two variables are opposite to the prediction of the deforestation scenario but consistent with previous analyses of rainfall (Easterling 2000; Houghton et al. 1998) and OLR (Chu et al. 1994). As depicted by Krishnamurti (1973) and Streten and Zillman (1984), the Amazon Basin is located at the root of an upward branch of the east–west circulation. Increasing trends of P and OLR over this basin may be coupled with the intensification of the east–west circulation and upward motion in this basin. This intensification may be reflected by the decreasing trend of surface pressure, p_s (Fig. 2d). Deforestation simulations suggest that T_s of the Amazon Basin may increase by 1°–3°C. The interdecadal trend of T_s (Fig. 2c) exhibits only a slight increase [consistent with Jones et al.'s (1999) analysis, but smaller than the range suggested by the deforestation scenario] in the past four decades. Interdecadal trends of P, OLR, p_s, and T_s of stations within the Amazon Basin suggest that the negative impact of deforestation on the hydrological processes in this basin, as predicted by numerous numerical studies, is overshadowed by interdecadal changes in the opposition due to features of the global circulation.

The interdecadal trends of station P, p_s, and T_s, and OLR in Fig. 2 lead to two questions: 1) Do these

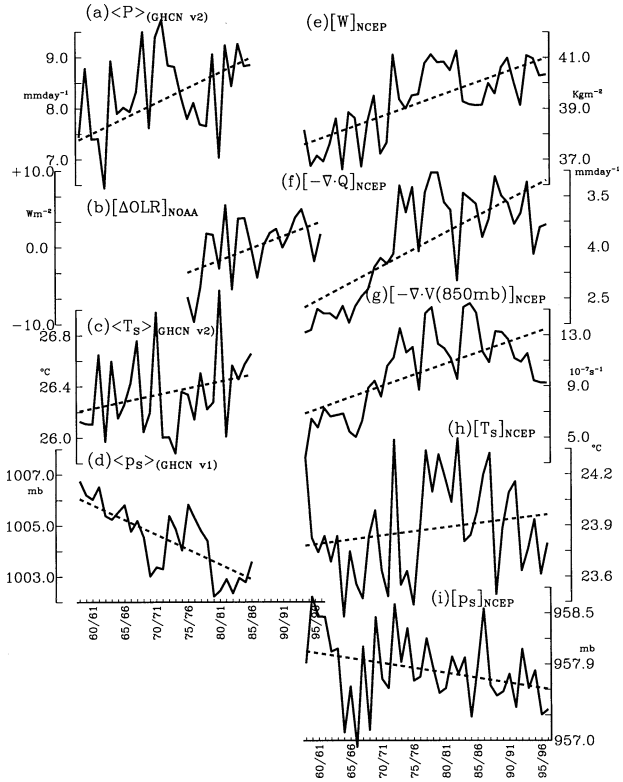

FIG. 2. Time series (solid lines) and interdecadal trends (straight dashed lines) of variable departures from their long-term summer-mean values derived from three datasets: 1) GHCN station observations: (a) precipitation (P), (c) surface temperature (T_s), and (d) surface pressures (p_s); 2) outgoing longwave radiation: (b) ΔOLR [= $\overline{\text{OLR}}$ – OLR; $\overline{\ }$ is a long-term summer-mean value of ( )]; and 3) NCEP–NCAR reanalysis data: (e) precipitable water (W), (f) convergence of water vapor flux ($-\nabla \cdot \boldsymbol{Q}$), (g) 850-mb horizontal convergence [$-\nabla \cdot \boldsymbol{V}$ (850 mb)], (h) surface temperature (T_s), and (i) surface pressure (p_s). The symbols < > and [ ] represent the algebraical average over all stations used and the area average over the analysis domain of 15°S–5°N, 70°–50°W, respectively.

interdecadal trends represent data bias? And 2) if not, what is the possible mechanism responsible for these trends? To answer these questions, we analyzed interdecadal trends of hydrological and surface variables with reanalysis data over the domain of 15°S–5°N, 70°–50°W embedded by the Amazon Basin. Any variable averaged over this domain is denoted by [ ]. The $[W]_{\text{NCEP}}$ trend (Fig. 2e) indicates that the basin became more moist over the past four decades in accordance with the $[P]_{\text{GHCN}}$ trend. Since sources of these two variables are independent, their concurrent increasing trends strongly indicate that the atmospheric branch of the basin's hydrological cycle has intensified. Previous studies (e.g., Salati and Nobre 1991; Eltahir and Bros 1994) argue that convergence of water vapor flux is not an effective means to maintain

Amazon rainfall. However, the basin convergence of water vapor flux $[-\nabla \cdot \boldsymbol{Q}]_{\mathrm{NCEP}}$ provides one more independent hydrological assessment for comparison with trends of $[P]_{\mathrm{GHCN}}$ and $[W]_{\mathrm{NCEP}}$. It turns out that $[-\nabla \cdot \boldsymbol{Q}]_{\mathrm{NCEP}}$ (Fig. 2f) also exhibits an increasing trend like the other two hydrological variables. These analyses strongly suggest that intensification of the Amazon hydrological cycle is not an artifact. Interdecadal trends of $[T_s]_{\mathrm{NCEP}}$ and $[p_s]_{\mathrm{NCEP}}$ are revealed from Figs. 2g and 2i, respectively. Mean values and the slopes of the trends of these two variables are smaller than their counterpart station observations. These discrepancies may be attributed to the fact that reanalysis values are obtained by averaging over the entire analysis domain, while station values are of only 14 stations. Nevertheless, trends of $[T_s]_{\mathrm{NCEP}}$ and $[p_s]_{\mathrm{NCEP}}$ confirm those of station observations within the basin. The possible intensification of the east–west circulation over the Amazon is also reflected by the $[p_s]_{\mathrm{NCEP}}$ trend in the NCEP reanalysis data.

The intensification of the east–west circulation with an upward branch located over the Amazon can be also reflected by the lower-tropospheric basin-scale horizontal convergence $[-\nabla \cdot \boldsymbol{V}(850\mathrm{mb})]_{\mathrm{NCEP}}$ (Fig. 2g). This result is consistent with trends of P, OLR, p_s, and T_s of stations within the Amazon Basin over this period. The increasing trend of this variable supports our speculation. Although the basin-scale convergence is regional, the east–west circulation centered over the Amazon Basin is linked to the global divergent circulation. It is likely that the intensification of the Amazon hydrological cycle by the interdecadal change of the global circulation is more than sufficient to compensate for the suppressive regional-scale mechanisms.

3. Possible mechanism

Divergences of mass flux ($\nabla \cdot \boldsymbol{V}$) and water vapor flux [$\nabla \cdot \boldsymbol{Q}$, where $\boldsymbol{Q} = (1/g)\int_o^{p_s} \boldsymbol{V} q dp$; g, p_s, $\boldsymbol{V}$, q, and p are gravity, surface pressure, velocity vector, specific humidity, and pressure, respectively] are local processes that can be linked to the global circulation through velocity potential (χ; Krishnamurti 1971) and potential function of water vapor flux (χ_Q; Chen 1985), respectively. Using horizontal distributions of (χ_Q, $\boldsymbol{Q}_D$) (where $\boldsymbol{Q}_{\mathrm{D}} = \nabla\chi_Q$, divergent component of water va-

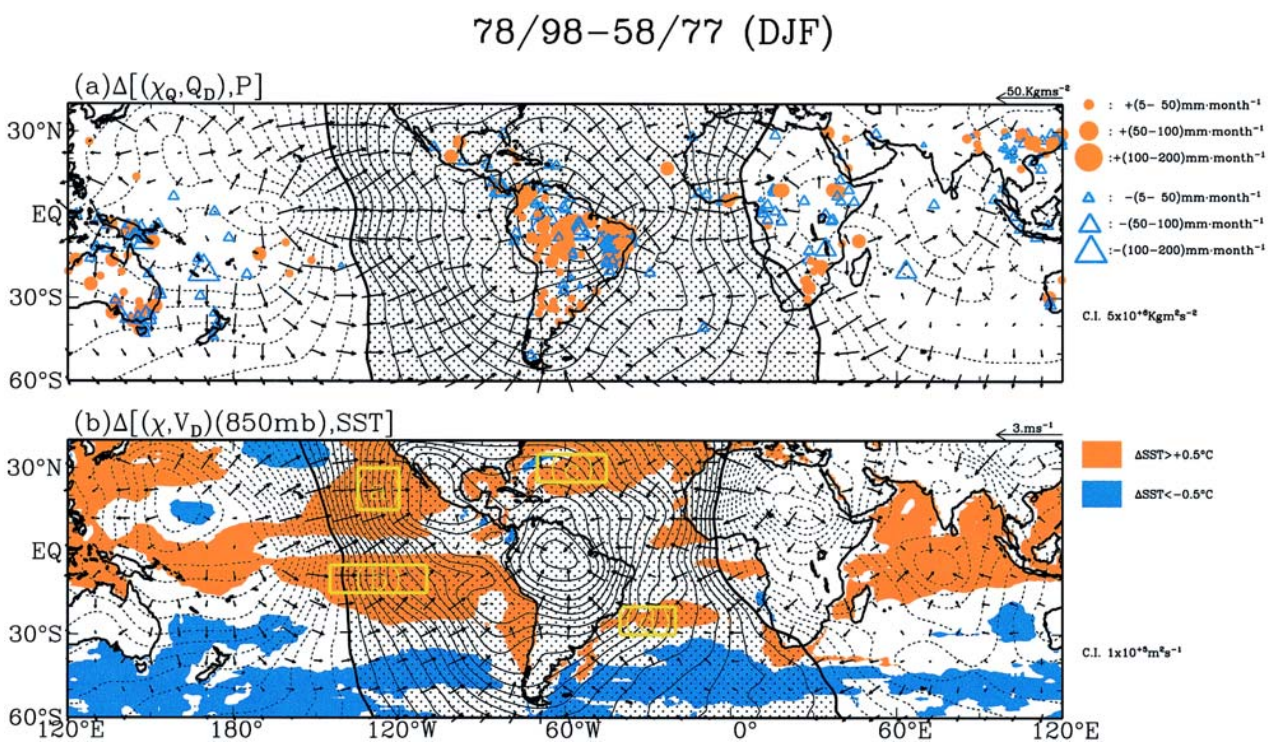

FIG. 3. Interdecacal changes [differences between the last (1978–98) and first (1958–77) two decades] of (a) $\Delta[\chi_Q, \boldsymbol{Q}_{\mathrm{D}}, P]$ and (b) $\Delta[(\chi, \boldsymbol{V}_{\mathrm{D}})$ (850 mb), SST]. Contour intervals of $\Delta\chi_Q$ and $\Delta\chi$(850 mb) are 5×10^6 kg m^2 s^{-1} and 10^5 m^2 s^{-1}, respectively. Positive value of $\Delta\chi_Q$ and $\Delta\chi$(850 mb) are lightly stippled. Values of ΔSST ≥ 0.5°C (≤ -0.5°C) are denoted by orange (blue), while values of $\Delta P \geq 0$ (≤ 0) are represented by different sizes of orange dots (open blue triangles).

por flux), Chen (1985) was able to demonstrate the maintenance of rainfall centers in the three tropical continents through the water vapor flux convergence driven by the east–west circulation. Thus, the increasing trend of rainfall and the suggested intensification of the east–west circulation associated with the upward motion over the Amazon Basin may be explained in terms of interdecadal changes in the χ_Q and lower-tropospheric χ fields over the entire globe. For illustration, differences of these two variables between the last and first two decades of 1958–99, $\Delta\chi_Q$ and $\Delta\chi$(850 mb), shown in Fig. 3, are used to illustrate how the interdecadal change of the global divergent circulation is related to the Amazon rainfall.

The $\Delta\chi_Q$ pattern (Fig. 3a) exhibits a wave 1 structure with a positive center located over the Amazon Basin. As indicated by $\Delta\boldsymbol{Q}_D$, water vapor converges toward this basin to maintain the increasing trends of $\Delta[W]$ and $\Delta[P]$ from the central-western Pacific in the west and the Indian Ocean–African continent in the east. The interdecadal change of the global divergent circulation in the lower troposphere is depicted by $\Delta(\chi, \boldsymbol{V}_D)$ (850 mb). The close pattern similarity between $\Delta(\chi, \boldsymbol{V}_D)$ (850 mb) and $\Delta(\chi_Q, \boldsymbol{Q}_D)$ indicates that the latter is primarily driven by the former. In turn, interdecadal increasing trends of $\Delta[W]$ and $\Delta[P]$ in the Amazon Basin may be responses of the regional hydrological cycle in this basin to the interdecadal change in the global divergent circulation. Then, what may be the possible mechanism causing this interdecadal change? A heuristic argument is offered below.

Numerous studies have been devoted to examining the interdecadal variation of winter circulation over the North Pacific (e.g., Chen et al. 1992; Latif and Barnett 1996) and the Northern Atlantic (e.g., Kushnir 1994; Hurrel 1995). Some recent efforts were also made to explore the possible impact of the interdecadal variation of the global circulation on the ENSO activity (e.g., Wang 1995). However, the interdecadal variation of the global divergent circulation during the northern winter and the possible cause of this variation have not been fully investigated. Interdecadal variations in sea surface temperature (SST) are always considered as a most likely cause of the interdecadal changes in the atmospheric circulation over the North Pacific and the North Atlantic. Can this be the case with the interdecadal change of the global divergent circulation? The ΔSST [SST (last two decades) – SST (first two decades)] anomalies are superimposed on $\Delta(\chi, \boldsymbol{V}_D)$ (850 mb) in Fig. 3b. The ΔSST time series over four regions (marked in Fig. 3b) are shown in Fig. 4. Increasing trends of SST in these regions suggest that the coherent interdecadal warming of oceans surrounding South America may be a possible cause of $\Delta(\chi, \boldsymbol{V}_D)$ (850 mb). This heuristic argument needs a numerical study to substantiate it. A study along this line is currently undertaken with the NCAR community climate model (CCM3) and the Goddard NASA Interannual-Seasonal Prediction Project climate model.

One may argue that ΔSST anomalies are also positive over the tropical and northwestern Pacific and the northern Indian Ocean. Why should there be a con-

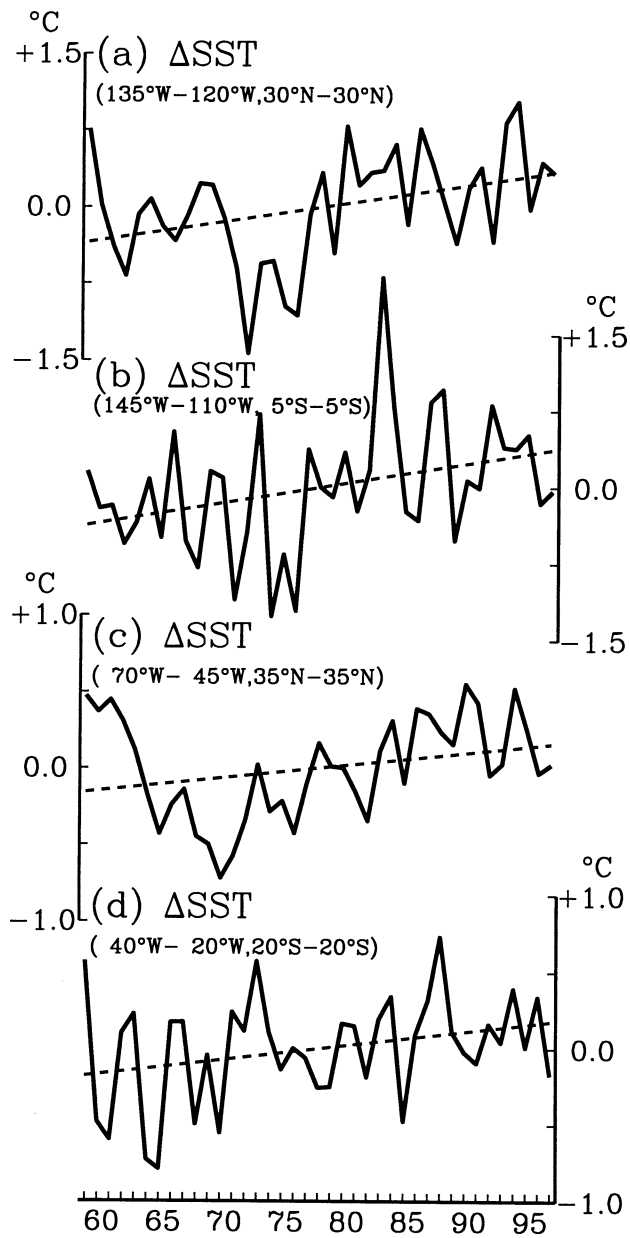

FIG. 4. Area-average ΔSST (SST departure from its long-term summer-mean value) over four areas encircled by yellow squares marked (a)–(d) on Fig. 3b.

vergent center in the lower troposphere over the Amazon, instead of the other side of the globe? Can this east–west hemispheric contrast of the interdecadal change in the global divergent circulation be a result of the east–west differentiation at the interdecadal warming, that is, the interdecadal warming over the hemisphere centered at the Amazon is more than the other hemisphere? To answer this question, the hemispheric-mean temperature departure at 925 mb, ΔT(925 mb), and the thickness (equivalent to the layer-mean temperature) departure between 850 and 200 mb, ΔZ(200–850 mb), from their four-decade mean values are shown in Fig. 5. As we can see, the slopes of both ΔT(925 mb) and ΔZ(200–850 mb) trends are larger in the Western Hemisphere than the Eastern Hemisphere. Evidently, the thermal contrast between the Eastern and Western Hemispheres is consistent with the $\Delta\chi$(850 mb) contrast between these two hemispheres. Conceivably, the faster interdecadal warming in the Western Hemisphere results in a convergent [$\Delta\chi$(850 mb) > 0] hemisphere centered in the Amazon.

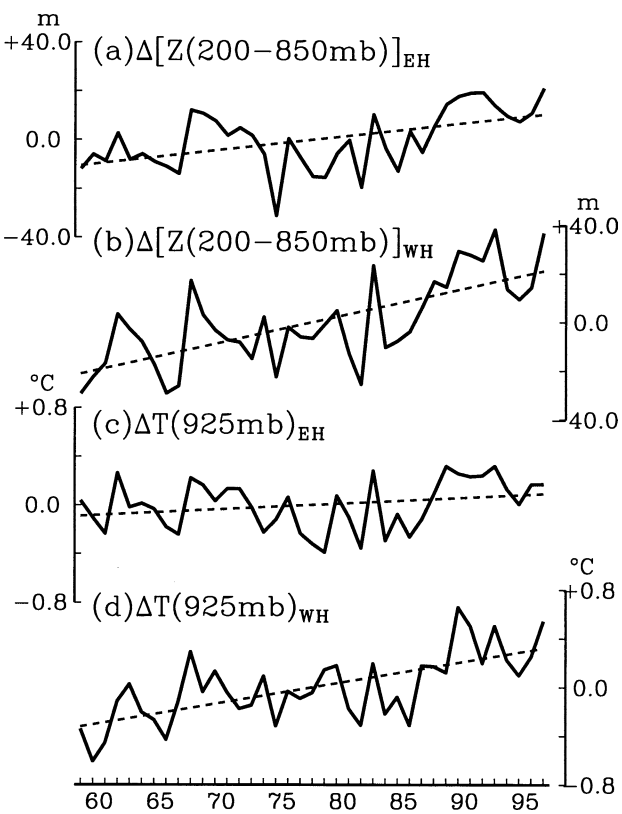

FIG. 5. Hemispheric-mean values of (a) ΔZ(200–850 mb), departure of thickness (between 200 and 850 mb) from its long-term summer-mean value, in the Eastern Hemisphere (EH), (b) ΔZ(200–850 mb) in the Western Hemisphere (WH), (c) ΔT(925 mb), 925-mb temperature departure from its long-term summer-mean value, in the EH, and (d) ΔSST (925 mb) in the WH.

4. Concluding remarks

The major findings of this study may be summarized as follows.

1) Rainfall in the Amazon Basin exhibits an increasing trend over the past four decades. Likewise, the atmospheric branch of the regional hydrological cycle in the basin has intensified and not weakened over this period.
2) The interdecadal change in the global divergent circulation has enhanced water vapor flux convergence toward the Amazon Basin of sufficient magnitude to counteract mesoscale drying that otherwise would be expected. The global divergent circulation is the dominating influence on the interdecadal change in the hydrological cycle of the basin. Interdecadal changes in Amazon Basin rainfall and hydrological cycle evidently are strongly linked to changes in the global divergent circulation.

These findings have relevance for research relating deforestation to regional climate change and to use of past modeling studies and use of past trends in ecosystem changes to formulate future strategy in dealing with deforestation and possible reforestation.

1) The observed trend toward increased precipitation in the Amazon Basin resulting from the increase in global divergent circulation perhaps has suppressed the full, and either positive or negative, regional or global climatic impact of deforestation. Future sensitivity studies of the climatic impact of deforestation must take into account long-term global circulation changes in order to evaluate the full range of possible impacts of land use. For instance, increased rainfall over the last 40 years may have led to enhanced regenerative growth in abandoned deforested land and reforested land compared to the impacts of a decreasing precipitation trend, as suggested without consideration of global circulation changes. On the other hand, enhanced rainfall on deforested soils may have exacerbated soil erosion and led to enhanced land degradation over what might have occurred in the absence of global-circulation-enhanced precipitation. Furthermore, the 20% increase in precipitation over the last

40 years could have changed the competitive advantage for certain plant species directly through climate change and indirectly through favoring different insect or pathogen species. Nutrient cycling and potential for carbon sequestration could have been altered by precipitation changes of this magnitude. Therefore, full accounting for the causes of ecological changes in deforested areas of Amazonia in the past 40 years should include changes in the global circulation as well as direct and indirect effects of deforestation.

2) Uncertainties about possible future changes in the global divergent circulation on decadal timescales call for a wider class of studies on the potential impacts of deforestation under a full range of plausible global circulation patterns. Past computer simulation analyses of deforestation impacts were based on differences between two types of simulations: *control* and *deforestation.* Most deforestation simulations have been short (perhaps only several years), so the interdecadal variation of the atmospheric circulation in response to variations of SST (even when "real" SSTs are used) are not included. Our findings strongly suggest that future numerical experiments over the Amazon Basin should include both major factors influencing the gradual climate change in the area: deforestation and interdecadal variation of the global divergent circulation.

The Atmospheric Modeling Intercomparison Project (Gates 1992) was developed as a systematic means of assessing capabilities of current global climate models. Perhaps a systematic, multimodel simulation that includes these global circulation effects should be used as a follow-up to the regional modeling studies that already have been done to evaluate the range of possible climatic implications of deforestation.

Acknowledgments. This study is supported by NSF Grant ATM-9906454 and NASA Grant NAG5-8293. The typing support provided by Mrs. Reatha Diedrichs is highly appreciated.

References

Avissar, R., and Y. Liu, 1996: Three-dimensional numerical study of shallow convective clouds and precipitation induced by land surface forcings. *J. Geophys. Res.,* **101** (D3), 7499–7518.

Brubaker, K., D. Entekhabi, and P. S. Eagleson, 1993: Estimation of continental precipitation recycling. *J. Climate,* **6,** 1077–1089.

Chen, T.-C., 1985: Global water vapor flux and maintenance during FGGE. *Mon. Wea. Rev.,* **113,** 1801–1819.

——, H. Van Loon, K.-D. Wu, and M.-C. Yen, 1992: Changes in the atmospheric circulation over the North Pacific–North America area since 1950. *J. Meteor. Soc. Japan,* **70,** 1137–1145.

——, J.-M. Chen, and C. K. Wikle, 1996: Interdecadal variation in the U.S. Pacific Coast precipitation over the past four decades. *Bull. Amer. Meteor. Soc.,* **77,** 1197–1205.

Chu, P.-S., Z.-P. Yu, and S. Hastenrath, 1994: Detecting climate change concurrent with deforestation in the Amazon Basin: Which way has it gone? *Bull. Amer. Meteor. Soc.,* **75,** 579–583.

Dickinson, R. E., and A. Henderson-Sellers, 1988: Modeling tropical deforestation: A study of GCM land-surface parameterizations. *Quart. J. Roy. Meteor. Soc.,* **114,** 439–462.

Easterling, D. R., T. C. Peterson, and T. R. Karl, 1996: On the development and use of homogenized climate datasets. *J. Climate,* **9,** 1429–1434.

——, T. R. Karl, K. P. Gallo, D. A. Robinson, K. E. Trenberth, and A. Dai, 2000: Observed climate variability and change of relevance to the biosphere. *J. Geophys. Res.,* **105** (D15), 20 101–20 114.

Eltahir, E. A. B., and R. L. Bras, 1994: Precipitation recycling in the Amazon Basin. *Quart. J. Roy. Meteor. Soc.,* **120,** 861–880.

Fearnside, P. M., 1987: Causes of deforestation in the Brazilian Amazon. *The Geophysiology of Amazonia,* R. E. Dickinson, Ed., Wiley, 37–61.

——, 1990: The rate and extent of deforestation in Brazilian Amazonia. *Environ. Conserv.,* **17,** 213–229.

Gates, W. L., 1992: AMIP: The Atmospheric Model Intercomparison Project. *Bull. Amer. Meteor. Soc.,* **73,** 1962–1970.

Henderson-Sellers, A. T. B. Durbidge, A. J. Pitman, R. E. Dickinson, P. J. Kennedy, and K. McGuffie, 1993: Tropical deforestation: Modeling local- to regional-scale climate change. *J. Geophys. Res.,* **98** (D4), 7289–7315.

Houghton, J. T., L. G. Meira Filho, B. A. Callander, N. Harris, A. Kaltenerg, and K. Maskell, 1996: *Climate Change 1998: The Science of Climate Change.* Cambridge University Press, 572 pp.

Hurrel, J. W., 1995: Decadal trends in the North Atlantic Oscillation regional temperature and precipitation. *Science,* **269,** 676–679.

Instituto Nacional de Pesquisas Espaciais, 1989: Avaliacao da cobertura florestal na Amazonia Legal Utilizando Sensoriamento Remoto Orbitat INPE, San Jose dos Campos, SP, Brazil.

Jones, P. D., M. New, D. E. Parker, S. Martin, and I. G. Rigor, 1999: Surface air temperature and its changes over the past 150 years. *Rev. Geophys.,* **37,** 173–200.

Kalnay, E., and Coauthors, 1996: The NCEP/NCAR 40-Year Reanalysis Project. *Bull. Amer. Meteor. Soc.,* **77,** 437–471.

Krishnamurti, T. N., 1971: Tropical east–west circulation during the northern summer. *J. Atmos. Sci.,* **28,** 1342–1347.

——, M. Kanamitsu, W. J. Koss, and J. D. Lee, 1973: Tropical east–west circulations during the northern winter. *J. Atmos. Sci.,* **30,** 780–787.

Kushnir, Y., 1994: Interdecadal variations in North Atlantic sea surface temperature and associated atmospheric conditions. *J. Climate,* **7,** 142–157.

Latif, M., and T. Barnett, 1996: Decadal climate variability over the North Pacific and North America—Dynamics and predictability. *J. Climate,* **9,** 2407–2423.

Lean, J., C. B. Buntou, C. A. Nobre, and P. R. Rowntree, 1996: The simulated impact of Amazonian deforestation on climate using measured ABRACOS vegetation characteristics. *Amazonian Deforestation and Climate,* J. H. C. Gash et al., Eds., John Wiley, 549–476.

Liebman, B., and D. L. Hartmann, 1982: Interannual variations of outgoing IR associated with tropical circulation changes during 1974–78. *J. Atmos. Sci.,* **39,** 1153–1162.

Nobre, C. A., P. J. Sellers, and J. Shukla, 1991: Amazonian deforestation and regional climate change. *J. Climate,* **4,** 957–988.

Peterson, T. C., and R. S. Vose, 1997: An overview of the Global Historical Climatology Network temperature database. *Bull. Amer. Meteor. Soc.,* **78,** 2837–2849.

Salati, E., and C. A. Nobre, 1991: Possible climate impacts of tropical deforestation. *Climate Change,* **19,** 177–196.

Shukla, J., C. A. Nobre, and P. J. Sellers, 1990: Amazonian deforestation and climate change. *Science,* **247,** 1322–1325.

Skole, D. L., W. Chomentowski, and C. A. Nobre, 1990: New estimates of Amazonian deforestation in the late 1970s using a Geographic Information System. Center for Complex Systems Research, University of New Hampshire, Durham, NH.

Smith, T. M., and R. W. Reynolds, 1998: A high-resolution global sea surface temperature climatology for the 1961–90 based period. *J. Climate,* **11,** 3320–3323.

Streten, N. A., and J. W. Zillman, 1984: Climate of the South Pacific Ocean. *Climate of the Oceans.* H. van Loon, Ed., Vol. 15, *World Survey of Climatology,* Elsevier, 263–430.

Sud, Y. C., G. K. Walker, J.-H. Kim, G. E. Liston, P. J., Sellers, and K. M. Lau, 1996: Biogeographical consequences of a tropical deforestation scenario: A GCM simulation study. *J. Climate,* **9,** 3225–3247.

Trenberth, K. E., 1999: Atmospheric moisture recycling: Role of advection and local evaporation. *J. Climate,* **12,** 1368–1381.

Vose, R. S., R. O. Schmoyer, P. M. Steurer, T. C. Peterson, R. Heim, T. R. Karl, and J. Eischeid, 1992: The Global Historical Climatology Network: Long-term monthly temperature, precipitation, sea level pressure, and station pressure data. Tech. Rep. ORNL/CDIAC-53, NDP-041. Carbon Dioxide Information Analysis Center, Oak Ridge National Laboratory, Oak Ridge, TN.

Wang, B., 1995: Interdecadal changes in El Niño onset in the last four decades. *J. Climate,* **8,** 267–285.

Xie, P., and P. A. Arkin, 1997: Global precipitation: A 17-year monthly analysis based upon gauge observations, satellite estimates, and numerical model outputs. *Bull. Amer. Meteor. Soc.,* **78,** 2539–2558.